

The Use of rAAV2-*RB1*-Mediated Gene Therapy in Retinoblastoma

Hanhan Shi,^{1,2} Xiaoyu He,^{1,2} Zhi Yang,^{1,2} Qili Liao,^{1,2} Jing Ruan,^{1,2} Shengfang Ge,^{1,2} Peiwei Chai,^{1,2} Renbing Jia,^{1,2} Jiayan Fan,^{1,2} Xuyang Wen,^{1,2} and Xianqun Fan^{1,2}

¹Department of Ophthalmology, Shanghai Key Laboratory of Orbital Diseases and Ocular Oncology, Shanghai Ninth People's Hospital, Shanghai JiaoTong University School of Medicine, Shanghai, People's Republic of China

²Shanghai Key Laboratory of Orbital Diseases and Ocular Oncology, Shanghai, People's Republic of China

Correspondence: Xianqun Fan, Ninth People's Hospital, Shanghai JiaoTong University School of Medicine, No.639, Zhizaoju Road, Huangpu District, Shanghai 200011, China; fanxq@sjtu.edu.cn.

Xuyang Wen, Ninth People's Hospital, Shanghai JiaoTong University School of Medicine, No.639, Zhizaoju Road, Huangpu District, Shanghai 200011, China; winston-a@hotmail.com.

Jiayan Fan, Ninth People's Hospital, Shanghai JiaoTong University School of Medicine, No.639, Zhizaoju Road, Huangpu District, Shanghai 200011, China; fanjiayan1118@126.com.

HS, XH, ZY, and QL contributed equally to this work.

Received: August 14, 2023

Accepted: November 23, 2023

Published: December 22, 2023

Citation: Shi H, He X, Yang Z, et al. The use of rAAV2-*RB1*-mediated gene therapy in retinoblastoma. *Invest Ophthalmol Vis Sci*. 2023;64(15):31.

<https://doi.org/10.1167/iovs.64.15.31>

PURPOSE. Retinoblastoma (RB) is a life-threatening malignancy that arises from the retina and is activated upon homozygous inactivation of the tumor suppressor *RB1*. Gene therapy targeting *RB1* is an effective strategy to treat RB. However, it is difficult to target the *RB1* gene by site-specific repair, with up to 3366 gene mutation sites identified in *RB1*. Thus, it is necessary to construct a promising and efficacious gene therapeutic strategy for patients with RB.

METHODS. To recover the function of the RB1 protein, we constructed a recombinant adeno-associated virus 2 (rAAV2) expressing RB1 that can restore RB1 function and significantly inhibit RB progression. To confirm the clinical feasibility of rAAV2-*RB1*, the RB1 protein was validated in vitro and in vivo after transfection. To further evaluate the clinical efficacy, RB patient-derived xenograft models were established and applied. The biosafety of rAAV2-*RB1* was also validated in immunocompetent mice.

RESULTS. rAAV2-*RB1* was a rAAV2 expressing the RB1 protein, which was validated in vitro and in vivo. In vitro, rAAV2-*RB1* was effectively expressed in patient-derived RB cells. In mice, intravitreal administration of rAAV2-*RB1* in a population-based patient-derived xenograft trial induced limited tumor growth. Moreover, after transfection of rAAV2-*RB1* in immunocompetent mice, rAAV2-*RB1* did not replicate and was expressed in other important organs, except retinas, inducing minor local side effects.

CONCLUSIONS. Our study suggested a promising efficacy gene therapeutic strategy, which might provide a chemotherapy-independent treatment option for RB.

Keywords: *RB1*, gene therapy, AAV, PDX

Retinoblastoma (RB), a tumor of the developing retina, is the most common pediatric eye cancer and an important cause of childhood death, and an estimated 8000 cases of RB are diagnosed each year worldwide.^{1,2} Despite considerable improvements in systemic drug delivery approaches and new administration routes, such as intravitreal and intraocular artery administration, severe visual impairment and eye loss are still frequent because of the toxicity associated with chemotherapeutic agents and the development of chemoresistance.³⁻⁵ Thus, it is important and urgent to focus on identifying new targeted therapies with improved antitumor activity and a lower risk of resistance.

A better understanding of the biology and genetics of RB will provide more therapeutic leads.^{6,7} Biallelic inactivation of *RB1*, located on chromosome 13 (13q14.2), in a susceptible retinal progenitor cell is the most common cause of

RB.⁸⁻¹¹ Approximately 40% of RB cases are hereditary and manifest as bilateral multifocal disease, and the other 60% of cases are nonheritable, feature local biallelic *RB1* inactivation in the developing retina, and involve only one eye.¹² The two-hit hypothesis on the *RB1* gene is considered an irreversible process of RB occurrence. As an important tumor suppressor gene, *RB1*'s functional deficiency still plays an important role in the development of RB. Previous studies have suggested that subsequent aberrations are needed for further malignant transformation.¹³⁻¹⁵ Dysfunction of the RB protein (RB1) in retinal cells promotes uncontrolled cell division and oncogenesis in RB.^{10,16} Therefore, *RB1* is not only considered a trigger for RB occurrence, but also a potential target for RB treatment.

Gene therapy is a novel therapeutic strategy for patients with RB and is mainly used for the treatment of diseases



related to single gene mutations.¹⁷ Through gene replacement or gene editing technology, normal genes are introduced into human cells to treat diseases caused by genetic defects; such strategies precisely target the root cause of these diseases—abnormal DNA—and can often achieve better results than traditional treatments.^{18,19} Currently, there have been significant advances in gene therapy in the clinic, and more than 40 gene therapy drugs have been approved by the U.S. Food and Drug Administration for marketing worldwide. Because of the very high number of *RB1* mutation sites and diverse *RB1* mutation types, it is difficult to restore the function of *RB1* with precise DNA repair.²⁰ Thus, the construction of a safe and efficient vector to supplement *RB1* is key for successful gene therapy for RB. Adeno-associated virus (AAV) can widely and selectively infect tissues and cells with low immunogenicity and integration and relatively high delivery efficiency and safety.^{21–23} AAV-mediated gene therapy has been applied in the clinic for other diseases and has achieved encouraging results.^{24,25} Interestingly, as the world's first U.S. Food and Drug Administration–approved AAV-based gene therapy drug, voretigene neparvovec (Luxturna), supplements the RPE65 gene to treat Leber congenital amaurosis.²² The successful application of voretigene neparvovec suggests the effectiveness and clinical transformation potential of AAV as a gene delivery tool.

Here, we constructed an RB gene therapy system using *RB1* as the target and AAV as the delivery vehicle to achieve precise and targeted gene therapy, and we assessed its safety. This system is expected to be a novel therapeutic strategy that can be used to improve the rate of eye preservation and the visual prognosis of children with RB.

METHODS

Sample Collection and Ethical Approval

This study was conducted in accordance with Declaration of Helsinki and approval of the Institutional Review Board of the Shanghai Ninth People's Hospital, Shanghai Jiao Tong University School of Medicine (SH9H-2019-T185-2). Written informed consent was obtained from each patient's parents. Human tumor specimens were obtained from patients who had undergone surgical eye removal.

DNA Sequencing

Fresh frozen tumor tissues ($n = 5$) were obtained from the biospecimen bank of Ninth People's Hospital, Shanghai Jiao Tong University School of Medicine, tumor DNA was extracted and prepared for whole-exome sequencing. Whole-exome sequencing was carried out using a TWIST Comprehensive Exon kit (102033, Twist Bioscience) and an Illumina NovaSeq6000, with sequencing performed at a depth of 60×. Clean reads were aligned against the human reference genome hs37d5 (based on GRCh37 assembly with human virus sequences) with default parameters. Mutect2 in GATK3.7 was used to detect possible single nucleotide variations and small insertions or deletions in the tumor genome. Significantly mutated genes, regarded as candidates for driver genes, were identified via the MutSigCV tool using mutations in all samples as the input and comparing them against the background mutation rate.

Patient-Derived Xenograft Animal Model Experiments

All mouse experiments were approved by the Animal Experimental Ethics Committee at Ninth People's Hospital, Shanghai Jiao Tong University School of Medicine (SH9H-2023-A774-1). A total of 4×10^5 cells for the patient-derived xenograft (PDX) model were implanted on the retinas through intraocular injection to establish a stable orthotopic RB model in BALB/c nude mice (female, 4–5 weeks old). The eyeball volume was calculated by the formula volume = length (mm) × width (mm)²/2. The eyeballs of each mouse were measured every 7 days for 28 consecutive days. PDX animals were randomly assigned to the recombinant AAV 2 (rAAV2)-*RB1* and empty vector groups. The investigators were blinded to the animal identity in the data analysis.

Production of Virus

Recombinant AAV2-*RB1* was packaged by Vigene Biosciences (Rockville, MD, USA). Specially, C-terminal Flag-tagged *RB1* was cloned and inserted into the AAV plasmid containing the cytomegalovirus promoter, which was flanked by AAV2-inverted terminal repeats. All AAV serotype vectors were produced in HEK 293T cells cotransfected with the rep-cap fused plasmid and a helper plasmid. AAVs were purified by iodixanol gradient ultracentrifugation. In brief, cultured medium was collected twice every 48 h after transfection. The cell lysate was treated with chloroform, and the supernatant was collected. The medium and supernatant were combined and concentrated by precipitation with 10% PEG 8000 and 1.0 M NaCl at 4°C overnight. After centrifugation, the pellet was resuspended in 1 × PBS buffer with benzonase. Iodixanol solutions (15%, 25%, 40%, and 60%) were carefully layered and then the generated viral suspension was overlaid, followed by centrifugation at 350,000×g for 90 minutes at 10°C. After ultracentrifugation, the AAV-containing 40% fraction was collected. The buffer was exchanged to remove the iodixanol and concentrate the purified virus. The amplified sequences are presented in Supplementary Table S1.

Intravitreal Injection of rAAV2-*RB1* Serotypes

Intravitreal injection was performed using a micropipette, which was inserted immediately behind the superotemporal limbus through the sclera into the vitreous cavity. One microliter of viral particles was injected into the vitreous cavity.

Quantitative Real-Time PCR

Total RNA was extracted from samples using an EZ-press RNA purification kit (B0004), and cDNA was generated using a PrimeScript RT reagent kit (Takara Bio Kusatsu, Shiga, Japan). Quantitative real-time PCR was performed using Powerup SYBR Green PCR Master Mix (Life Technologies, Carlsbad, CA, USA) on a real-time PCR system (Applied Biosystems, Waltham, MA, USA). The primers are listed in Supplementary Table S2.

Western Blot Analysis

Tissues and cells were harvested and lysed with lysis buffer. The concentration of total protein was measured using a

bicinchoninic acid protein assay kit (Beyotime Institute of Biotechnology, Jiangsu, China). Protein samples were separated by sodium dodecyl sulfate-polyacrylamide gel electrophoresis in 7.5% (w/v) polyacrylamide gels and transferred to polyvinylidene fluoride membranes (Millipore, Bedford, MA, USA). After blocking with 5% milk for 1 hour at room temperature, the membranes were incubated with 2.5 µg/mL primary antibody in 5% BSA overnight at 4°C and then with the corresponding secondary antibody-conjugated to a fluorescent tag (Invitrogen, Waltham, MA, USA). The membranes were visualized with an Odyssey Infrared Imaging System (LI-COR, Lincoln, NE, USA).

Histology and Immunostaining

The tumor tissues were fixed with 4% formaldehyde (Thermo Fisher Scientific, Waltham, MA, USA), embedded in paraffin, and examined for tumor formation through histologic analysis of hematoxylin and eosin-stained sections. For immunohistochemistry, tumor slides were deparaffinized and rehydrated, and antigen retrieval was performed with an alcohol series and sodium citrate buffer. After blocking with 5% normal goat serum (Vector Laboratories, Inc, Newark, CA, USA) with 0.1% Triton X-100 and 3% H₂O₂ in PBS for 60 minutes at room temperature and incubation with primary antibodies at 4°C overnight, tissue slides were incubated with horseradish peroxidase conjugates using 3,3'-diaminobenzidine detection. Immunostaining was performed using the appropriate primary and secondary antibodies. Nuclei were counterstained with DAPI. Images were taken with a ZEISS Axio Scope A1 Upright Microscope (Carl Zeiss Meditec, Jena, Germany).

Electroretinography

A full-field ERG test was performed in mice with dark adaptation for 24 hours. The mice were anesthetized with isoflurane (induction: 3% at 1.0 L min⁻¹; maintenance: 1.5% at 0.6 L min⁻¹; Suzhou Kunchen Biotechnology Co., Ltd, Suzhou, China). Then, the pupils of the mice were enlarged by topical administration of 2.5% phenylephrine containing 0.5% tropicamide. Then, a ground electrode was placed on the tail of a mouse, a reference electrode was installed on the forehead of the mouse, and a pair of 3-mm gold ring electrodes was placed on the cornea of the mouse. The responses of rod cells and cone cells to light stimulation were recorded using an Espion E3 machine (Diagnosys, LLC, Lowell, MA, USA). The intensity of 10 cd s m⁻² in a flash stimulation excited the scotopic ERG, the intensity of 30 cd s m⁻² was used to induce the photopic ERG, and then the light adaptation was carried out at an intensity of 10 cd s m⁻² for 5 minutes.

TABLE. Clinical Details of Patient-Derived RB PDX Models

Sample	<i>RB1</i> Mutation	PDX Models	Age at Diagnosis (Months)	Age at Enucleation (Months)	Laterality	Chemo Therapy
Patient 01	c.2307dupG; p.L769fs; frameshift insertion	PDX 01	16	17	Bilateral	No
Patient 02	c.C1981T; p.R661W; nonsense	PDX 02	68	68	Unilateral	No
Patient 03	Exon 1; gross deletion	PDX 03	36	36	Unilateral	No
Patient 04	c.370_371del; p.I124fs; frameshift deletion	PDX 04	20	20	Unilateral	No
Patient 05	c.608-478(IVS6)C>A; single nucleotide variation	PDX 05	54	56	Unilateral	No

Statistical Analyses

All statistical analyses were performed using Graphpad Prism software (Graphpad, Boston, MA, USA). Two-sided Student's *t* test and one-way ANOVA were used for data comparison. All tests were 2-sided, and a *P* value of less than 0.05 was considered statistically significant.

RESULTS

Clinical Features and Genetic Characteristics of Patients With RB

Between September 2021 and September 2022, five patients with RB were diagnosed with group E advanced RB with endophytic tumor growth at our center. Enucleation was the primary treatment without any other treatments. The patients' detailed clinical characteristics are summarized in Table. After enucleation, the resected tumor tissues were trimmed, and then the BALB/c mice received intraocular injection (Fig. 1A). After parental written informed consent for the patients was obtained, whole-exome sequencing was conducted on all five patients to systematically interrogate the genetic background of patients with RB from our center. *RB1* mutations at different locations were identified in all five patients, suggesting the potential for gene therapy (Fig. 1B, Table). To our knowledge, loss function of *RB1* is the most important cause of RB. Hence, we conducted Western blotting to detect the expression of *RB1* in patients' RB tissues. Notably, all patients with RB were validated to lack *RB1* expression (Fig. 1C).

Tumorigenicity of PDX In Vivo

Because the cells for the PDX model were implanted on the retinas through intraocular injection, fundography and optical coherence tomography imaging were used to monitor the intraocular grafts and evaluate the tumorigenicity of the PDX. At 1 week postinjection, all mice with PDXs showed visible tumors in the intraocular grafts. As further confirmed by hematoxylin and eosin staining (Fig. 1D), these results demonstrate that the PDXs could remain viable and expand in immunodeficient mice.

Retinal and Cellular Transduction by rAAV2-RB1

Next, we sought to examine the retinal transduction efficacy of rAAV2-*RB1*. In theory, the maximum loading capacity of AAV2 is 4.7 kb, whereas the *RB1* gene is 196 kb in length and includes 27 exons, hindering the development of gene therapy for RB. Hence, we deleted the intron

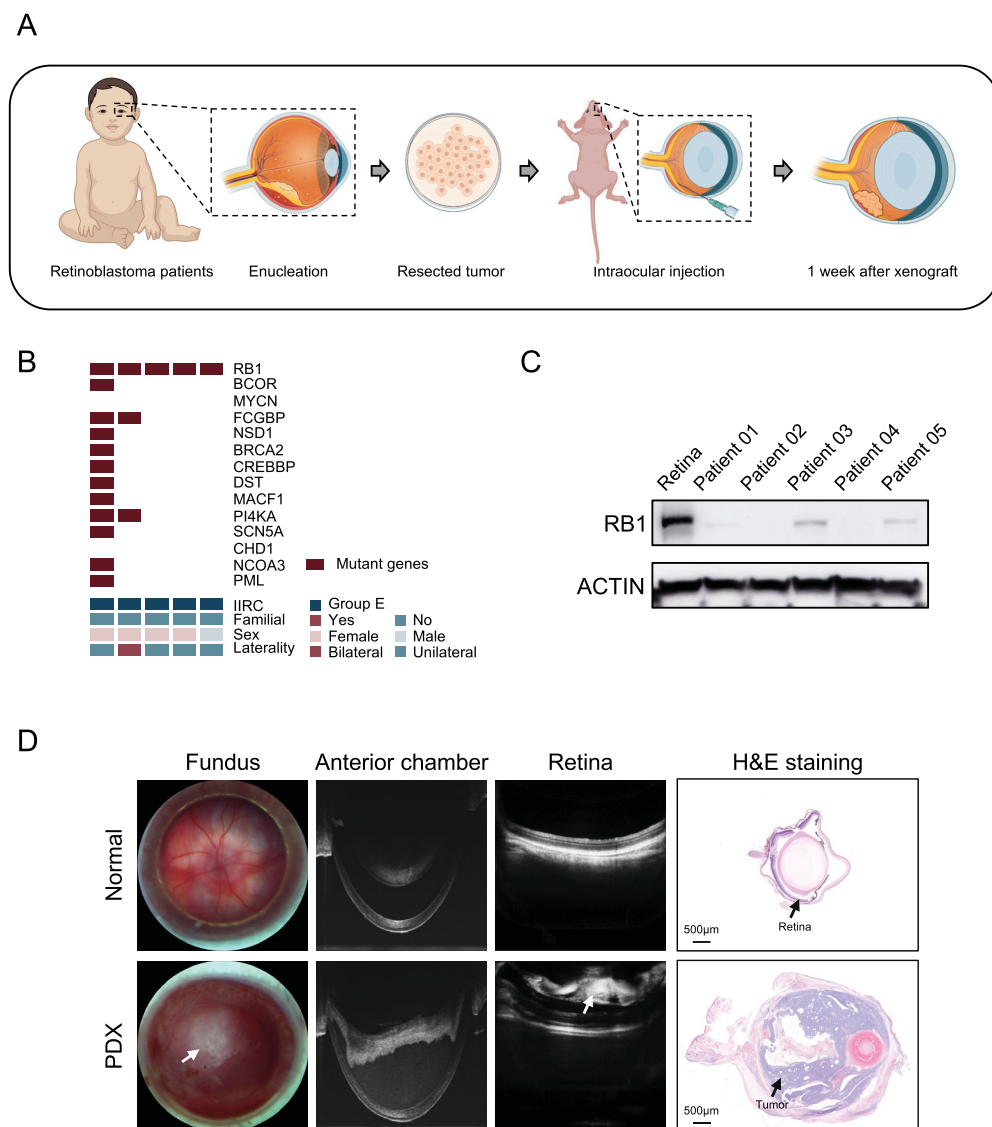


FIGURE 1. Establishment of the RB PDX model. **(A)** Stepwise schematic of the RB PDX model development. **(B)** Genomic landscape of 5 patients with RB in this study. **(C)** Western blot analysis showing RB1 expression in normal retina tissues and RB patient samples. **(D)** Ophthalmic examination of mouse eyes after subretinal engraftment. Representative fundus photograph of the anterior chamber and optical coherence tomography images of an eye with a patient tumor-derived xenograft (*bottom*) showing an obvious RB tumor in the retina. The other eye did not receive treatment and served as a normal control (*top*). The *white arrows* indicate tumors. Representative hematoxylin and eosin staining of eyes containing PDX and normal eyes to demonstrate pathological characteristics (*right*).

of *RB1* and loaded the new sequence into a recombinant AAV vector (rAAV2-*RB1*) (Fig. 2A). To test the cellular transduction efficiencies of rAAV2-*RB1*, we used patient-derived RB cells and found that after transduction by rAAV2-*RB1*, *RB1* was upregulated 20- to 30-fold (Fig. 2B). Moreover, *RB1* expression was also significantly upregulated (Fig. 2C).

We used intravitreal injection to validate the transduction efficacy of rAAV2-*RB1* in vivo by detecting the expression level of *RB1* in retinal tissues. As seen in our models, rAAV2-*RB1* showed penetration into the retina layer and was detected in the retina, (Fig. 2D). These results showed that rAAV2-*RB1* transcytosis occurred in the retinal layer, the central substrate of the blood-retinal barrier.

Evaluation of rAAV2-*RB1* in a Population-Based PDX Trial

RB is the most common malignant eye cancer in children, and novel therapeutic strategies are needed to improve ocular preservation. However, even after numerous therapies have been administered, surgical removal of the eye is sometimes performed to prevent extraocular metastases, which may be fatal.²⁶ Here, we applied rAAV2-*RB1* in an RB PDX cohort to validate its antitumor efficacy. Seven days after implantation of RB tumor cells from patients, rAAV2-*RB1* (1×10^{12} vg each; $n = 4$) and empty vector ($n = 4$) were administered intravitreally. The appearance of intravitreal tumors was visually assessed on day 7. The mice were sacrificed and the eyeballs in both groups

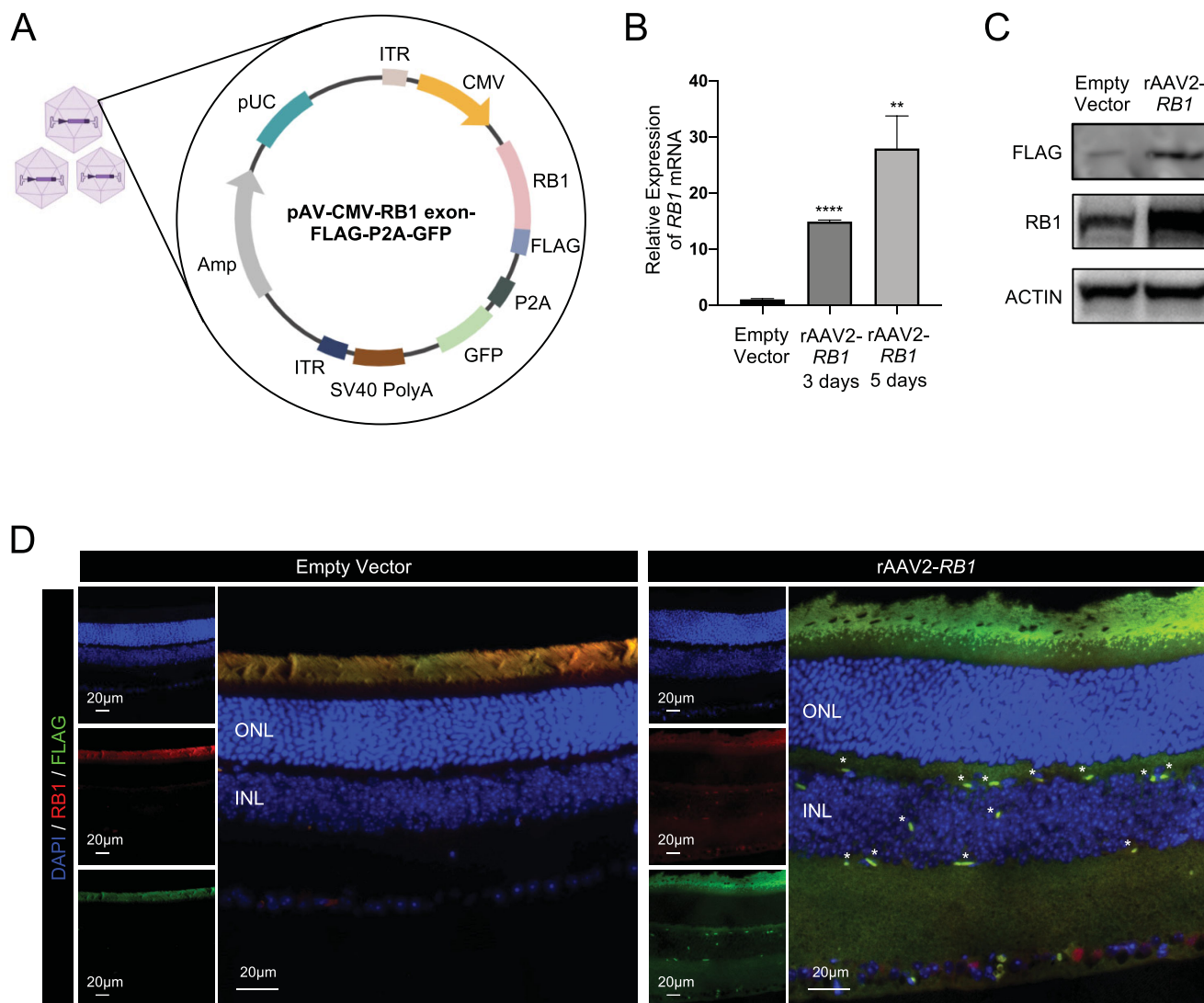


FIGURE 2. Cellular and retinal transduction by rAAV2-*RB1*. (A) Plasmid map of rAAV2-*RB1*. (B) Statistical results of *RB1* expression in rAAV2-*RB1*-treated and empty vector-treated patient-derived RB cells. Rates are shown as the mean \pm SD, * $P < 0.05$, ** $P < 0.01$, **** $P < 0.001$. (C) Western blot analysis showing *RB1* expression in rAAV2-*RB1*-treated and empty vector-treated patient-derived RB cells. (D) Immunostaining of *RB1* and rAAV2-*RB1* (FLAG) in rAAV2-*RB1*-treated and empty vector-treated mouse retinas. *Characteristic expression pattern of rAAV-*RB1*.

were collected on day 31. Immunofluorescence ($n = 1$), Western blotting ($n = 2$), and quantitative real-time PCR ($n = 1$) were separately performed to confirm rAAV2-*RB1*-mediated RNA and protein expression of *RB1* at the tumor site (Fig. 3A). When comparing the appearance of eyeballs from each PDX on day 7 and day 28, rapid tumor growth, bleeding, and rupture were observed in empty vector-treated animals, whereas limited growth and even the disappearance of tumor tissues were observed in rAAV2-*RB1*-treated animals (Fig. 3B). The appearance of tumor tissues after extraction of each PDX clearly illustrated the antitumor efficacy of rAAV2-*RB1* gene therapy (Fig. 3C). After treatment with rAAV2-*RB1*, the weight of tumor tissues was much lower than that of tumor tissues from empty vector-treated animals (Fig. 3D). Moreover, the growth of RB tumors was assessed, and tumor growth was decreased dramatically after injection of rAAV2-*RB1*

(Fig. 3E). These results suggest that rAAV2-*RB1* provides a considerable antitumor benefit in RB PDX tumor-bearing mice.

Histological examination at the end of the study revealed upregulated expression of *RB1* protein in tumor tissues after tumor implantation and rAAV2-*RB1* treatment (Fig. 4A). Increased expression of *RB1* and *RB1* protein was further observed in tumor tissue treated with rAAV2-*RB1* by RT-qPCR and Western blotting, respectively (Figs. 4B and 4C).

Activation of the immune system against viral coat proteins contributes to local adverse events related to adenovirus administration, as well as to AAV administration.²⁷ Thus, to characterize the toxicity of rAAV2-*RB1* in immunocompetent mice, we administered rAAV2-*RB1* (1×10^{12} vg per animal) to *C57BL/6* mice and subsequently examined the biosafety 24 days after administration of rAAV2-*RB1*. The treatment exhibited mild

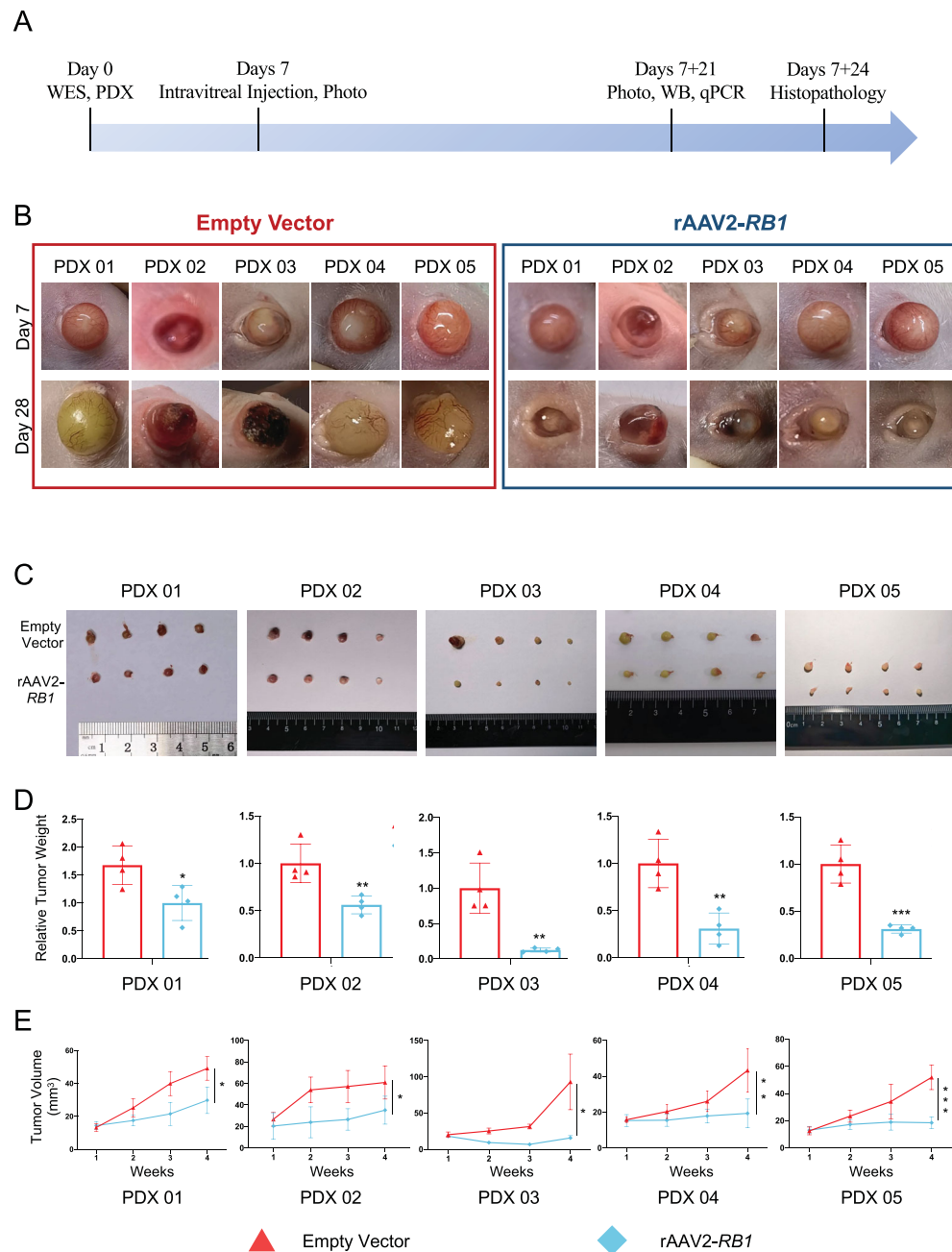


FIGURE 3. Efficacy of rAAV2-RB1 in a PDX model. **(A)** Schematic diagram of the study design including treatment, sampling, and efficacy assessment. PDX mice were randomly divided into two groups and then received intravitreal injections of equal concentrations (1×10^{12} vg) of rAAV2-RB1 and empty vector. **(B)** Representative photographs of engrafted eyes at 21 days after intravitreal injection. Empty vector-injected eyes showed tumor progression (*top*), while rAAV2-RB1-treated eyes showed limited tumor burden (*bottom*). **(C)** Representative eyeballs from empty vector- and rAAV2-RB1-treated mice in each PDX cohort. Rates are shown as the mean \pm SD, * $P < 0.05$, ** $P < 0.01$, *** $P < 0.001$. **(D)** Representative tumor weights from empty vector- and rAAV2-RB1-treated mice in each PDX cohort. Rates are shown as the mean \pm SD, * $P < 0.05$, ** $P < 0.01$, *** $P < 0.001$. **(E)** Representative volumes (mm^3) of eyeballs from empty vector- and rAAV2-RB1-treated mice on different days after intravitreal injection in each PDX cohort. Rates are shown as the mean \pm SD, * $P < 0.05$, ** $P < 0.01$, *** $P < 0.001$.

toxicity, both systemically and locally in mice. Intravitreal rAAV2-RB1 did not induce systemic symptoms in immunocompetent mice. At necropsy, the microscopic structures of the collected organs were normal, and flag staining was negative in all cases, indicating that there was no viral replication in off-target organs (Fig. 5A).

For local structures, pathological characteristics of eyeballs in saline solution-, empty vector-, and rAAV2-RB1-treated mice were exhibited without damage (Fig. 5B). To further explore the visual damage of rAAV2-RB1, ERG was conducted to test the visual function. There was no visual damage after rAAV2-RB1 administration (Fig. 5C).

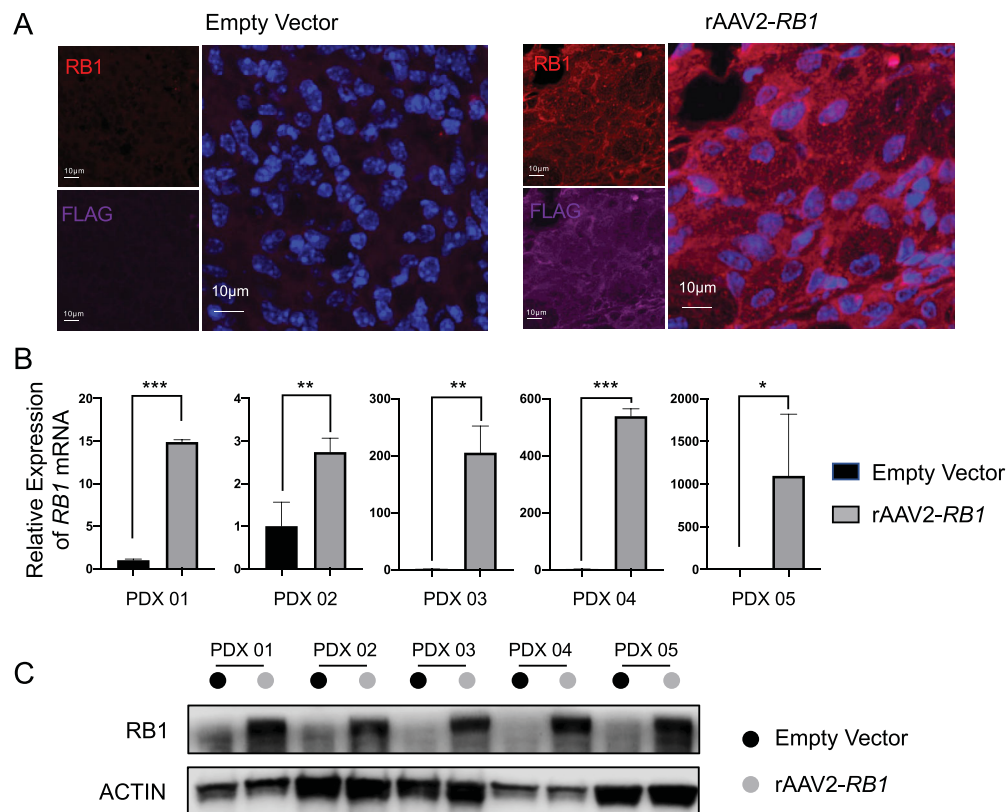


FIGURE 4. Evaluation of *RB1* expression in rAAV2-*RB1*-treated mice. (A) Immunostaining of *RB1* and rAAV2-*RB1* (FLAG) in rAAV2-*RB1*-treated and empty vector-treated tumor tissues in PDX mice. (B) Statistical results of *RB1* expression in rAAV2-*RB1*-treated and empty vector-treated PDX tumor tissues. Rates are shown as the mean \pm SD, * $P < 0.05$, ** $P < 0.01$, *** $P < 0.001$. (C) Western blot analysis showing *RB1* expression in empty vector- and rAAV2-*RB1*-treated RB PDX samples (empty vector group in *black* and rAAV2-*RB1* group in *gray*).

DISCUSSION

Numerous therapeutic strategies have emerged, resulting in enhanced clinical outcomes. However, no gene therapy has been reported previously in RB. Hence, rAAV2-*RB1* is a novel option for patients with RB with promising efficacy in RB PDX models. In this study, we constructed an RB gene therapy system using *RB1* as the target and AAV as the delivery vehicle as a precise and targeted gene therapy and conducted a safety assessment.

In contrast with most cancers, the genetic changes that initiate RB are well defined. Specially, RB is the most studied single-gene mutation tumor, with up to 3366 *RB1* gene mutation sites identified. Mutations in *RB1* were detected in 94% of patients with RB, including stop-gain mutations in 39.8% of patients, isodisomy of chromosome 13q in 35.0% of patients, loss of heterozygosity of *RB1* in 18.5% of patients, splicing mutations in 19.4% of patients, homozygous deletion of *RB1* in 8.8% of patients, and chromothripsis involving the *RB1* locus in 8.8% of patients.²⁸ However, the RB protein is essential for accurate DNA replication, and it has emerged that this protein regulates the stage of the cell cycle.²⁹ Hence, repairing the *RB1* gene and replenishing the RB1 protein by gene therapy may induce the cone precursor to exit the cell cycle and inhibit the tumorigenesis of RB.

Because of the very high number of *RB1* gene mutation sites and mutation types, it is difficult to restore the function of the *RB1* gene by gene editing-based repair of specific sites with technologies such as CRISPR-Cas9. A safe

and efficient expression vector that can be used to repair the entire *RB1* gene needs to be developed to improve the effectiveness of targeting the *RB1* gene for RB treatment. Viral vectors are the main tool for gene therapy.²¹ However, the high rate of host genome integration and systemic and local toxicity hinder the clinical application of lentiviruses, even though lentiviral vectors are ideal for delivery of the *RB1* gene. AAV is considered the commonly used viral vector for gene therapy because of its low immunogenicity, integration ability, and efficient infection procedure.²⁴ Hence, we developed rAAV2-*RB1* to replace mutated *RB1*, which exhibited promising efficacy in an RB PDX model and may be useful for clinical treatment. In addition to viral vectors, VCN-01 is an oncolytic adenovirus designed to selectively target tumor cells with a high abundance of E2F-1, and it has achieved promising outcomes in a mouse model and a phase I clinical trial.³⁰ However, enucleation was also conducted for the first two patients with RB who were enrolled in the clinical trial and underwent VCN-01 treatment for various reasons.

The blood-retinal barrier, small size, and limited environment of the eyeball make it possible to achieve high transduction efficiency in ocular tissues with a small dose of AAV vectors, suggesting the usefulness of gene therapy for eyeball diseases.^{31,32} However, the delivery efficiency of the AAV vectors used in ocular surgery remains low, which has severely limited the therapeutic efficacy. rAAV is an optimized and modified AAV with a stronger affinity for specific tissue cells, such as retinal photoreceptors and pigment cells, allowing it to better deliver gene therapy.³²⁻³⁴

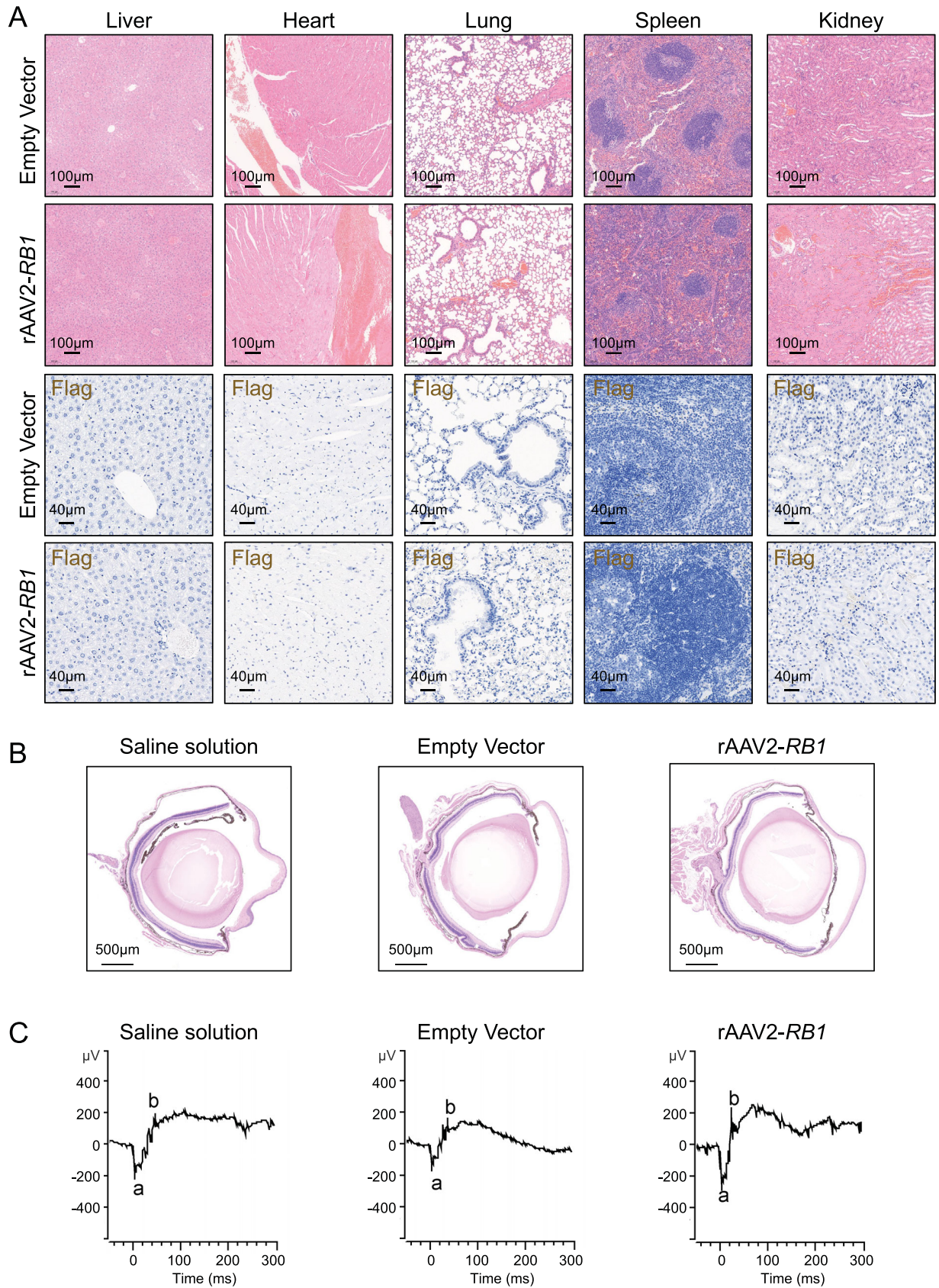


FIGURE 5. Evaluation of the systemic and local toxicity of rAAV2-RB1. **(A)** Pathological characteristics of essential organs in empty vector- and rAAV2-RB1-treated (*top*) mice. Immunohistochemical staining of empty vector- and rAAV2-RB1 (Flag) in essential organs of rAAV2-RB1-treated PDX mice (*bottom*). **(B)** Pathological structures of eyeballs in saline solution (*left*), empty vector (*middle*), and rAAV2-RB1-treated (*right*) mice. **(C)** Visual function of saline solution (*left*), empty vector (*middle*), and rAAV2-RB1-treated (*right*) mice evaluated by ERG at P10.

Although rAAV2-*RB1* exhibited promising efficacy in an RB PDX model, there is a long way to go before it can be applied in clinical treatment. rAAV2-*RB1* also lacks comparison with the current first-line treatment methods for RB (ophthalmic artery interventional chemotherapy, systemic venous chemotherapy, intraocular injection chemotherapy, etc.), and it is necessary to explore whether gene therapy with rAAV2-*RB1* and the combination of these first-line treatments can achieve greater benefits for patients with RB. In summary, we constructed a gene therapy system with *RB1* as the target and AAV as the delivery vehicle to achieve precise and targeted treatment for patients with RB. Intravitreal injection of rAAV2-*RB1* after RB patient tumor implantation produced a tumor-suppressive effect, and a safety evaluation was performed in an RB PDX model. rAAV2-*RB1* is thus a new potential therapy for patients with refractory RB, and it is expected to be a novel treatment for RB that will increase the rate of eye preservation and improve visual prognosis in children.

Acknowledgments

The authors thank to all patients with RB enrolled in our study and wish them good health.

Supported by grants from National Natural Science Foundation of China (grant 82272642, 82203260), The Science and Technology Commission of Shanghai (20DZ2270800, 20224Y0147, 23YF1422500), and Innovative research team of high-level local universities in Shanghai (SSMU-ZDCX20180401).

Disclosure: **H. Shi**, None; **X. He**, None; **Z. Yang**, None; **Q. Liao**, None; **J. Ruan**, None; **S. Ge**, None; **P. Chai**, None; **R. Jia**, None; **J. Fan**, None; **X. Wen**, None; **X. Fan**, None

References

- Global Retinoblastoma Study G, Fabian ID, Abdallah E, Abdullahi SU, et al. Global retinoblastoma presentation and analysis by national income level. *JAMA Oncol*. 2020;6:685–695.
- Chantada GL, Qaddoumi I, Canturk S, et al. Strategies to manage retinoblastoma in developing countries. *Pediatr Blood Cancer*. 2011;56:341–348.
- Abramson DH, Shields CL, Munier FL, Chantada GL. Treatment of retinoblastoma in 2015: agreement and disagreement. *JAMA Ophthalmol*. 2015;133:1341–1347.
- Pavlidou E, Burris C, Thaug C, et al. Anterior segment seeding in eyes with retinoblastoma failing to respond to intraocular chemotherapy. *JAMA Ophthalmol*. 2015;133:1455–1458.
- Grossniklaus HE. Retinoblastoma. Fifty years of progress. The LXXI Edward Jackson Memorial Lecture. *Am J Ophthalmol*. 2014;158:875–891.
- Zhang J, Benavente CA, McEvoy J, et al. A novel retinoblastoma therapy from genomic and epigenetic analyses. *Nature*. 2012;481:329–334.
- Dimaras H, Corson TW, Cobrinik D, et al. Retinoblastoma. *Nat Rev Dis Primers*. 2015;1:15021.
- Cavenee WK, Hansen MF, Nordenskjold M, et al. Genetic origin of mutations predisposing to retinoblastoma. *Science*. 1985;228:501–503.
- Friend SH, Bernards R, Rogelj S, et al. A human DNA segment with properties of the gene that predisposes to retinoblastoma and osteosarcoma. *Nature*. 1986;323:643–646.
- Xu XL, Singh HP, Wang L, et al. Rb suppresses human cone-precursor-derived retinoblastoma tumours. *Nature*. 2014;514:385–388.
- McEvoy J, Nagahawatte P, Finkelstein D, et al. RB1 gene inactivation by chromothripsis in human retinoblastoma. *Oncotarget*. 2014;5:438–450.
- Knudson AG, Jr. Mutation and cancer: statistical study of retinoblastoma. *Proc Natl Acad Sci USA*. 1971;68:820–823.
- Francis JH, Brodie SE, Marr B, Zabor EC, Mondesire-Crump I, Abramson DH. Efficacy and toxicity of intravitreal chemotherapy for retinoblastoma: four-year experience. *Ophthalmology*. 2017;124:488–495.
- Parareda A, Catala J, Carcaboso AM, et al. Intra-arterial chemotherapy for retinoblastoma. Challenges of a prospective study. *Acta Ophthalmol*. 2014;92:209–215.
- Wyse E, Handa JT, Friedman AD, Pearl MS. A review of the literature for intra-arterial chemotherapy used to treat retinoblastoma. *Pediatr Radiol*. 2016;46:1223–1233.
- Zhang J, Gray J, Wu L, et al. Rb regulates proliferation and rod photoreceptor development in the mouse retina. *Nat Genet*. 2004;36:351–360.
- Acland GM, Aguirre GD, Ray J, et al. Gene therapy restores vision in a canine model of childhood blindness. *Nat Genet*. 2001;28:92–95.
- Aposhian HV. The use of DNA for gene therapy—the need, experimental approach, and implications. *Perspect Biol Med*. 1970;14:98–108.
- Anzalone AV, Randolph PB, Davis JR, et al. Search-and-replace genome editing without double-strand breaks or donor DNA. *Nature*. 2019;576:149–157.
- Yao Y, Gu X, Xu X, Ge S, Jia R. Novel insights into RB1 mutation. *Cancer Lett*. 2022;547:215870.
- Kalesnykas G, Kokki E, Alasaarela L, et al. Comparative study of adeno-associated virus, adenovirus, baculovirus and lentivirus vectors for gene therapy of the eyes. *Curr Gene Ther*. 2017;17:235–247.
- Miraldi Utz V, Coussa RG, Antaki F, Traboulsi EI. Gene therapy for RPE65-related retinal disease. *Ophthalmic Genet*. 2018;39:671–677.
- Russell S, Bennett J, Wellman JA, et al. Efficacy and safety of voretigene neparvovec (AAV2-hRPE65v2) in patients with RPE65-mediated inherited retinal dystrophy: a randomised, controlled, open-label, phase 3 trial. *Lancet*. 2017;390:849–860.
- Mendell JR, Al-Zaidy SA, Rodino-Klapac LR, et al. Current clinical applications of in vivo gene therapy with AAVs. *Mol Ther*. 2021;29:464–488.
- Kuzmin DA, Shutova MV, Johnston NR, et al. The clinical landscape for AAV gene therapies. *Nat Rev Drug Discov*. 2021;20:173–174.
- Gunduz K, Muftuoglu O, Gunalp I, Unal E, Tacyildiz N. Metastatic retinoblastoma clinical features, treatment, and prognosis. *Ophthalmology*. 2006;113:1558–1566.
- Bessis N, GarciaCozar FJ, Boissier MC. Immune responses to gene therapy vectors: influence on vector function and effector mechanisms. *Gene Ther*. 2004;11(Suppl 1):S10–S17.
- Field MG, Kuznetsoff JN, Zhang MG, et al. RB1 loss triggers dependence on ESRRG in retinoblastoma. *Sci Adv*. 2022;8:eabm8466.
- Bosco G. Cell cycle: retinoblastoma, a trip organizer. *Nature*. 2010;466:1051–1052.
- Pascual-Pasto G, Bazan-Peregrino M, Olaciregui NG, et al. Therapeutic targeting of the RB1 pathway in retinoblastoma with the oncolytic adenovirus VCN-01. *Sci Transl Med*. 2019;11:eaat9321.
- Apte RS. Gene therapy for retinal degeneration. *Cell*. 2018;173:5.

32. Mochizuki M, Sugita S, Kamoi K. Immunological homeostasis of the eye. *Prog Retin Eye Res.* 2013;33:10–27.
33. Byrne LC, Day TP, Visel M, et al. In vivo-directed evolution of adeno-associated virus in the primate retina. *JCI Insight.* 2020;5:e135112
34. Dalkara D, Byrne LC, Klimczak RR, et al. In vivo-directed evolution of a new adeno-associated virus for therapeutic outer retinal gene delivery from the vitreous. *Sci Transl Med.* 2013;5:189ra176.